

Electronic Supplementary Information

Structure Reinforced Birnessite in Extended Potential Window for Supercapacitors

Yang Zhao,^{†^{a,b}} Qin Fang,^{†^a} Xiaohui Zhu,^{a,b} Liang Xue,^{a,b} Mingzhu Ni,^{a,b} Ce Qiu,^{a,b} Hao Huang,^{a,b} Shuo Sun,^{a,b} Shuang Li^a and Hui Xia^{*a,b}

^aSchool of Materials Science and Engineering, Nanjing University of Science and Technology, 210094 Nanjing, China.

^bHerbert Gleiter Institute of Nanoscience, Nanjing University of Science and Technology, 210094 Nanjing, China.

†Both authors contributed equally to this work.

Corresponding Author

*E-mail: xiahui@njust.edu.cn

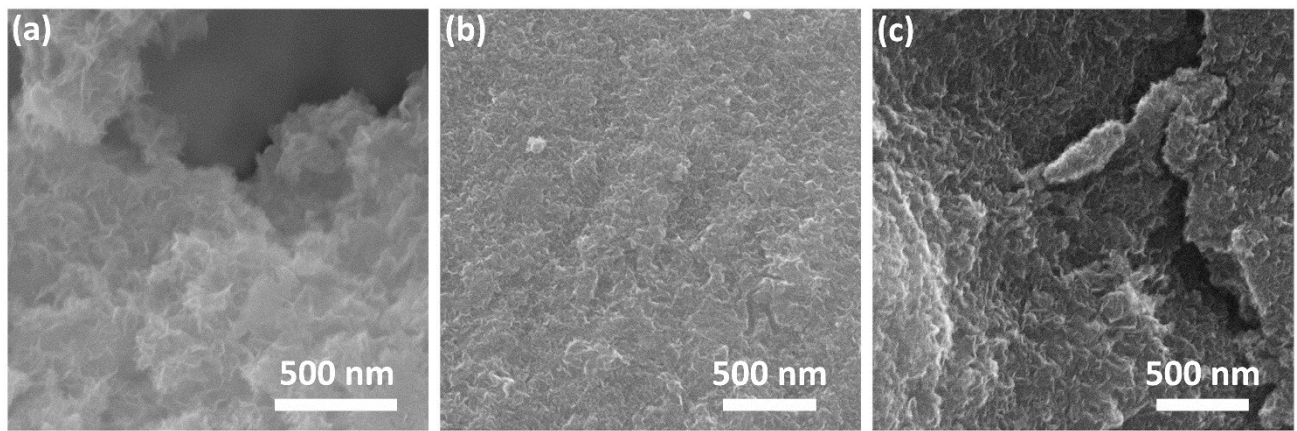


Figure S1. FESEM images of 0.01CrMO, 0.03CrMO and 0.05CrMO samples.

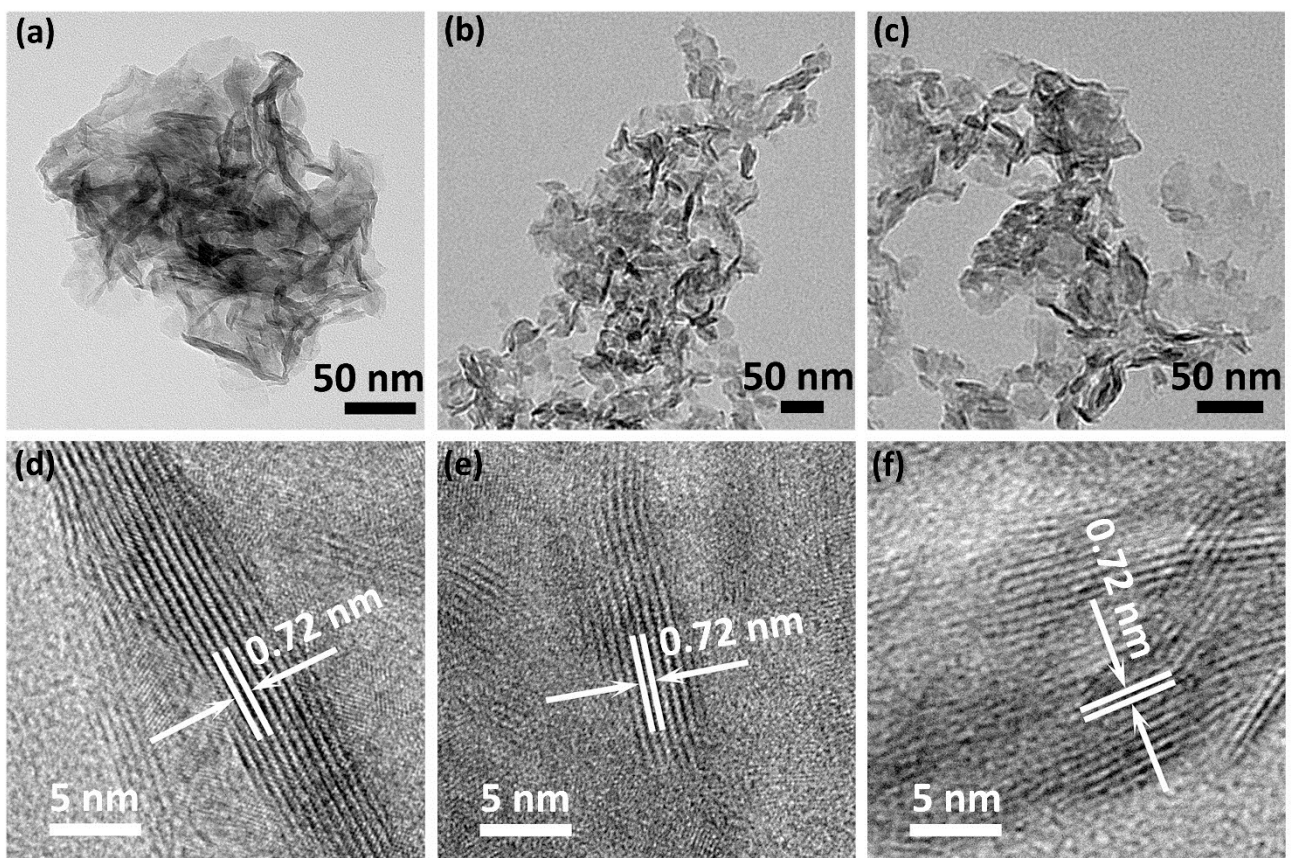


Figure S2. (a-c) TEM and (d-f) HRTEM images of 0.01CrMO, 0.03CrMO and 0.05CrMO samples.

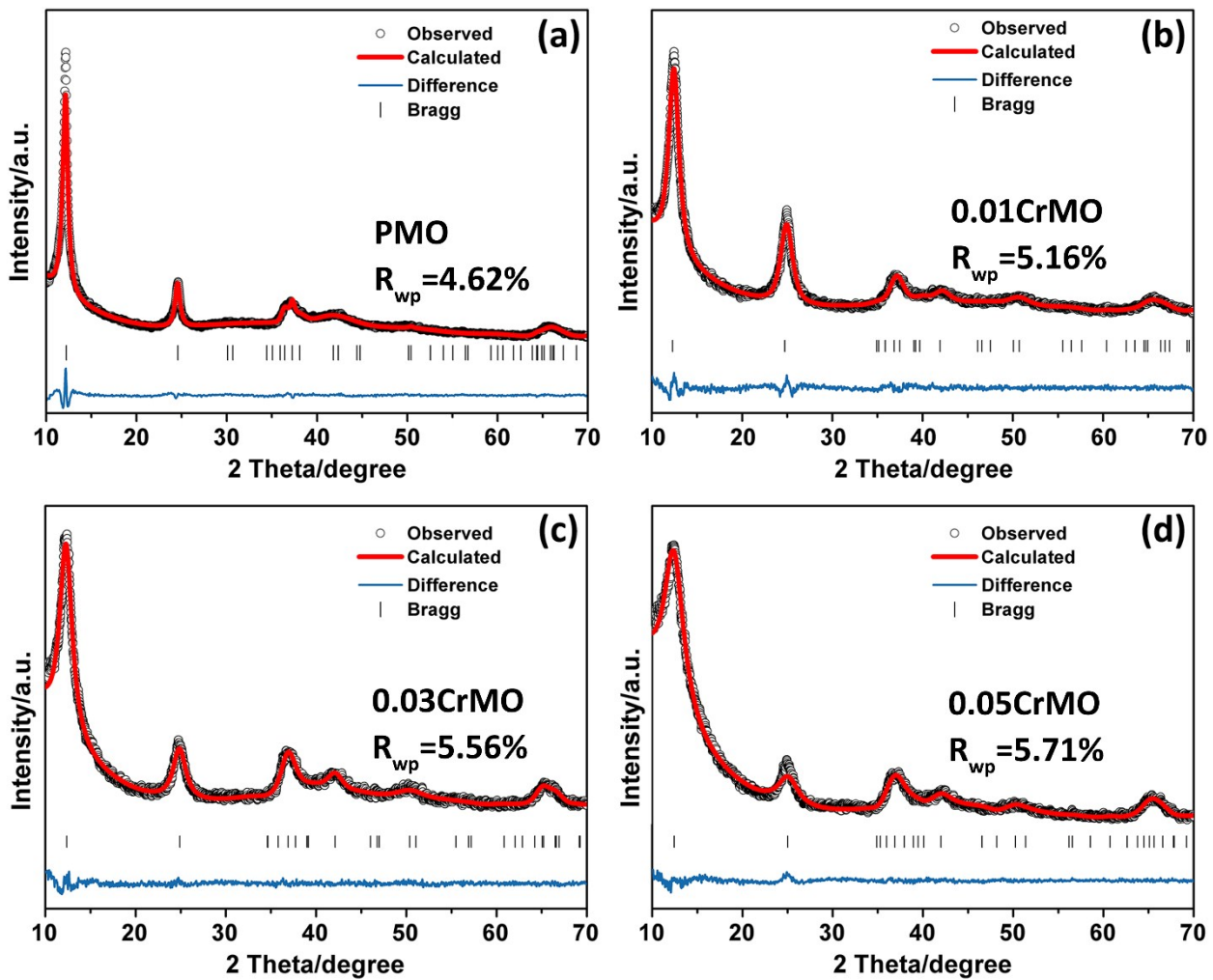


Figure S3. Rietveld refinements of the XRD patterns of the PMO (a), 0.01CrMO (b), 0.03CrMO (c), and 0.05CrMO (d) samples.

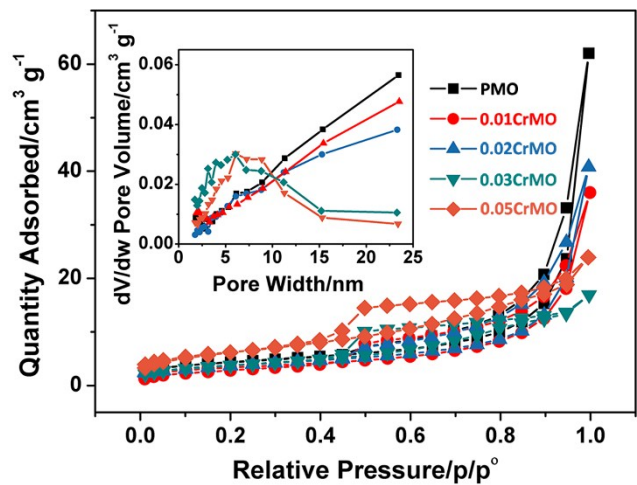


Figure S4. N₂ adsorption-desorption isotherms of the PMO, 0.01CrMO, 0.02CrMO, 0.03CrMO and 0.05CrMO samples. The inset shows the pore distributions for all samples.

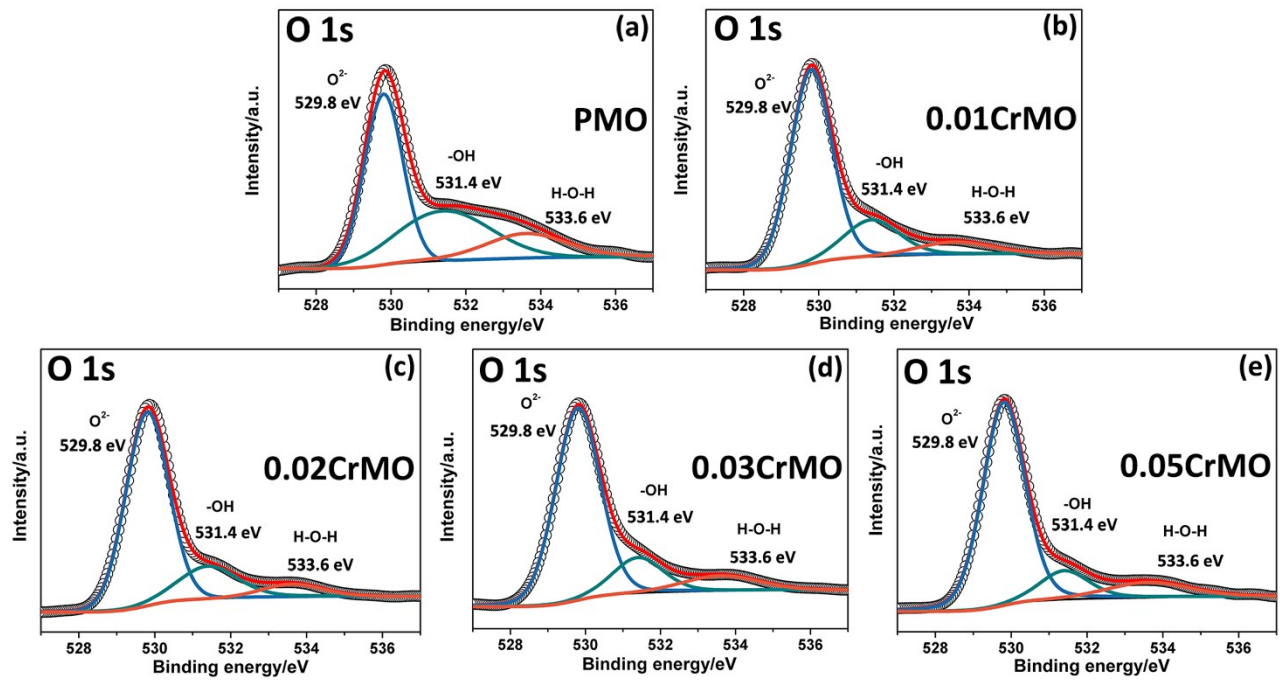


Figure S5. (a-e) High-resolution XPS spectra of O 1s of the PMO, 0.01CrMO, 0.02CrMO, 0.03CrMO and 0.05CrMO samples.

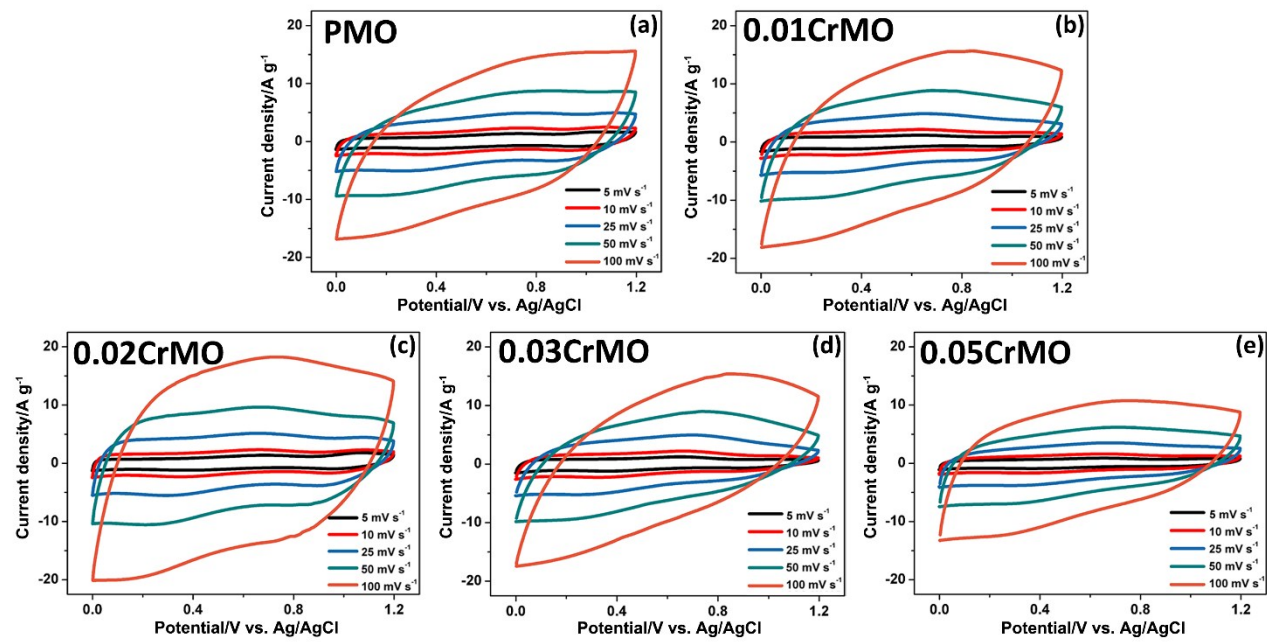


Figure S6. (a-e) CV curves of the PMO, 0.01CrMO, 0.02CrMO, 0.03CrMO and 0.05CrMO electrodes at different scan rates (5-100 mV s⁻¹).

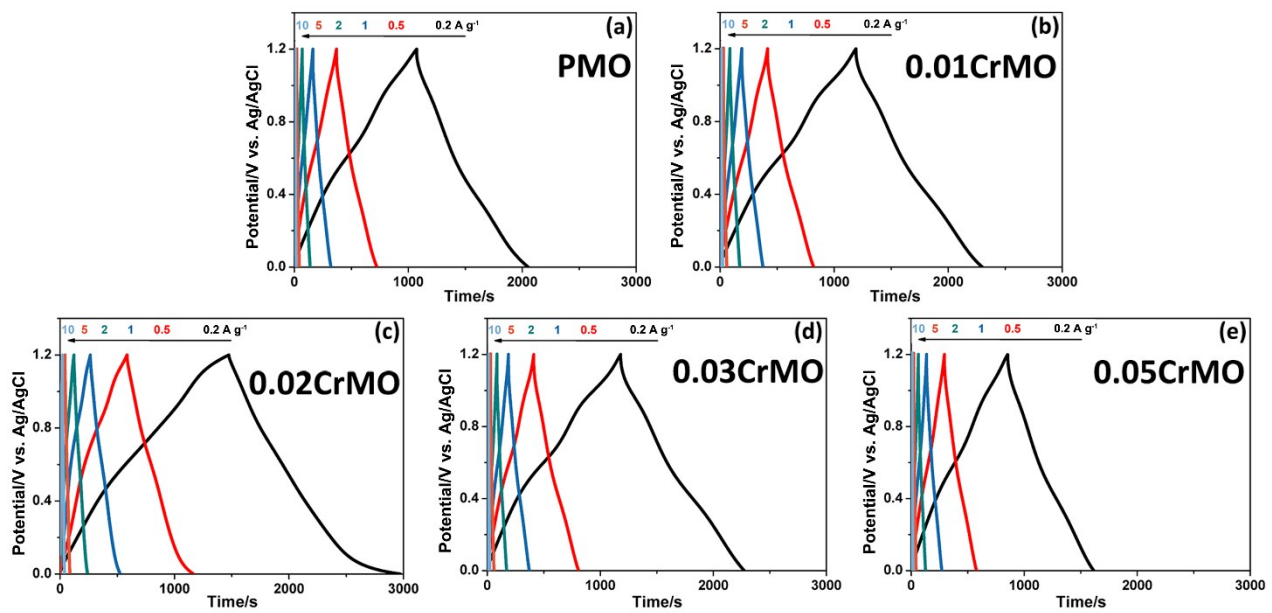


Figure S7. (a-e) GCD curves of the PMO, 0.01CrMO, 0.02CrMO, 0.03CrMO and 0.05CrMO electrodes at different current densities ($0.2\text{-}10\text{ A g}^{-1}$).

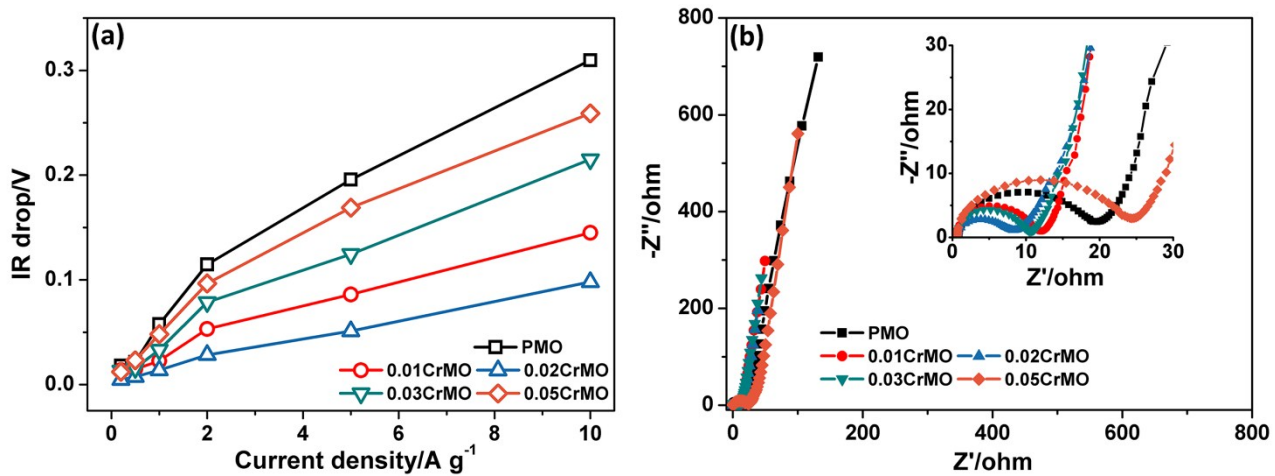


Figure S8. (a) IR drop as a function of current densities of the PMO, 0.01CrMO, 0.02CrMO, 0.03CrMO and 0.05CrMO electrodes. (b) EIS spectra of the PMO, 0.01CrMO, 0.02CrMO, 0.03CrMO and 0.05CrMO electrodes in a frequency range from 0.01 Hz to 100 kHz with a potential amplitude of 5 mV.

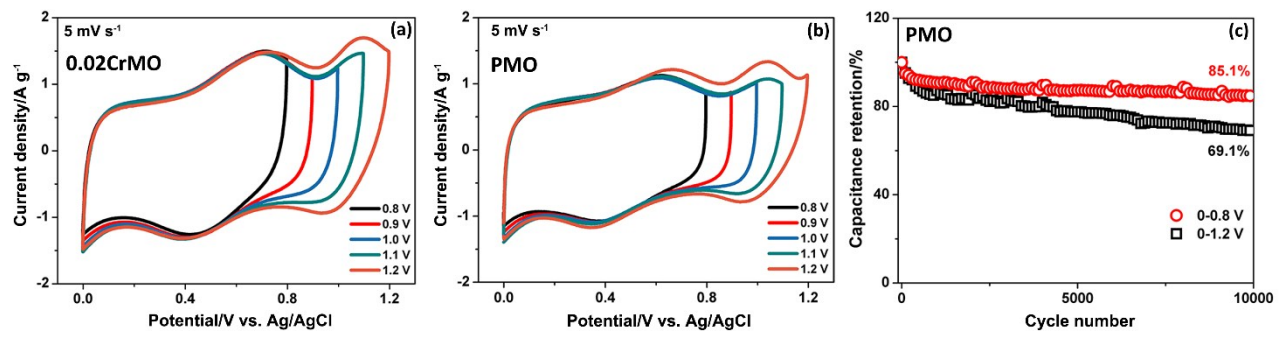


Figure S9. (a-b) CV curves of the 0.02CrMO and PMO electrodes in different potential windows of 0-0.8, 0-0.9, 0-1.0, 0-1.1 and 0-1.2 V (vs. Ag/AgCl) at 5 mV s^{-1} . (c) Cycle performances of the PMO electrode in the potential windows of 0-0.8 V and 0-1.2 V (vs. Ag/AgCl) at a current density of 10 A g^{-1} .

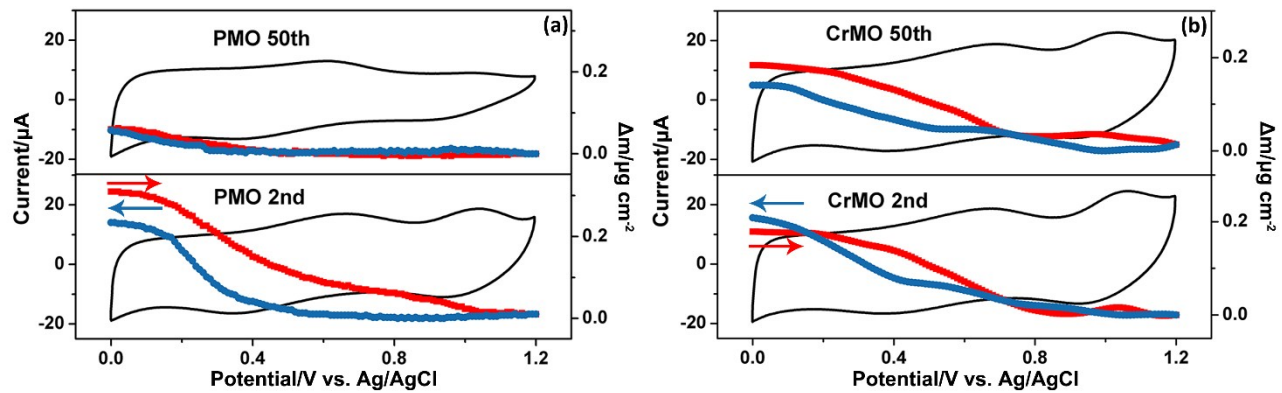


Figure S10. The CV curves and the corresponding Δm of the PMO (a) and 0.02CrMO (b) electrodes measured by EQCM.

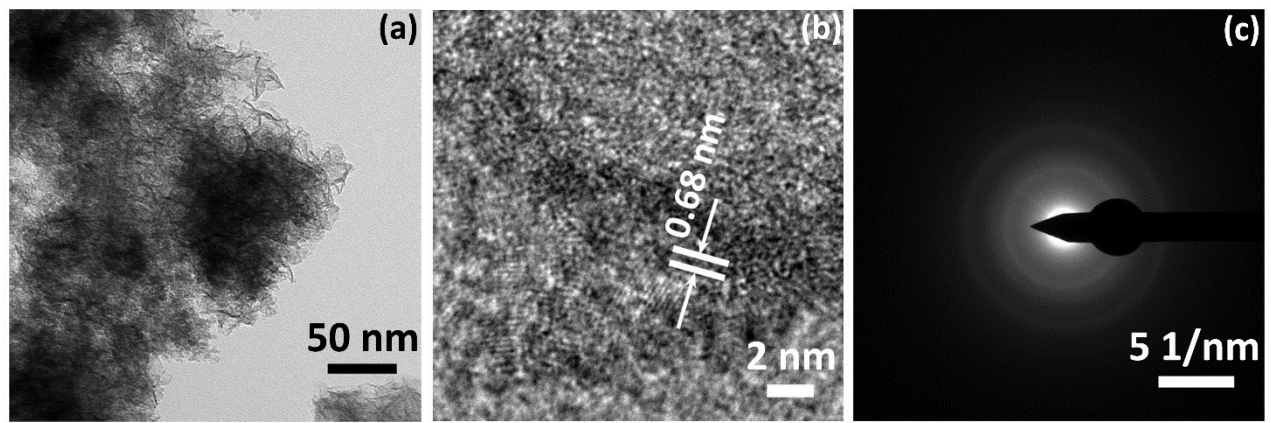


Figure S11. (a)TEM, (b)HRTEM images and (c) SAED pattern of precipitate in the electrolyte for PMO electrode.

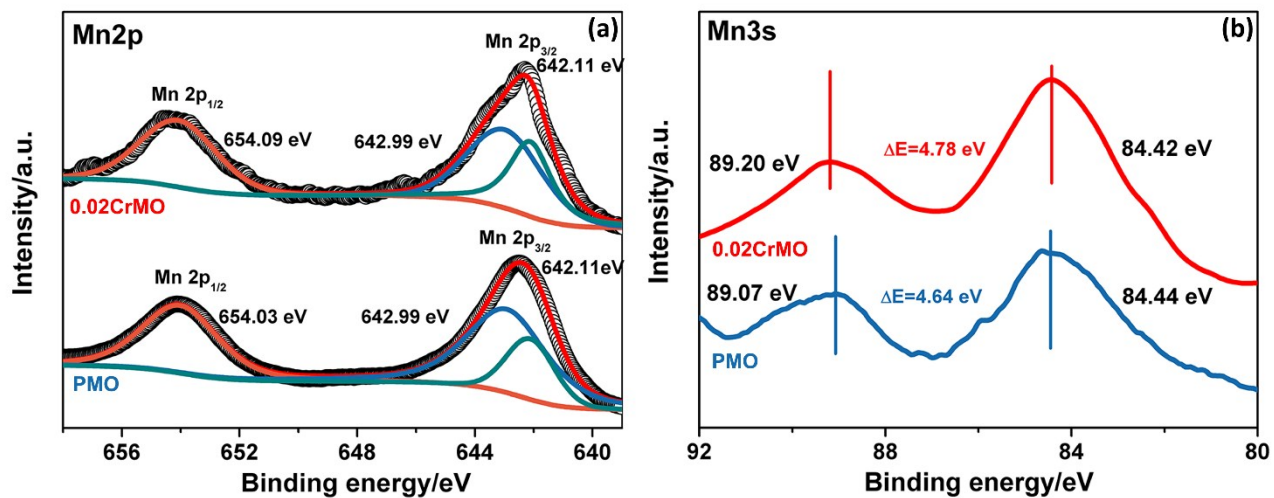


Figure S12. High-resolution XPS spectra of (a) Mn 2p and (b) Mn 3s of the PMO and 0.02CrMO electrodes after cycles.

Table S1. Lattice parameters determined using Rietveld refinement.

	PMO	0.01CrMO	0.02CrMO	0.03CrMO	0.05CrMO
a/Å	5.226	5.203	5.198	5.262	5.199
b/Å	2.848	2.869	2.851	2.865	2.863
c/Å	7.203	7.336	7.471	7.274	7.271
β/°	100.48	101.30	102.33	100.69	102.16
Mn-O bond length/Å	1.935/ 2.308	1.916/ 2.008	1.889/ 1.939	1.910/ 2.035	1.914/ 1.990

Table S2. The contents of element Na and Cr from ICP-OES measurements.

Samples	Atomic ratio	Atomic ratio
	Na/Mn	Cr/Mn
PMO	0.521	0
0.02CrMO	0.488	0.019

Table S3. The kinetic parameters of PMO, 0.01CrMO, 0.02CrMO, 0.03CrMO and 0.05CrMO electrodes.

	PMO	0.01CrMO	0.02CrMO	0.03CrMO	0.05CrMO
R_s/Ω	0.733	0.537	0.538	0.527	0.487
R_{ct}/Ω	15.981	10.012	6.378	8.716	19.982
$\sigma_w/\Omega \text{ Hz}^{1/2}$	6.885	3.986	3.707	4.563	7.421
$D_{\text{Na}^+}/10^{-10} \text{ cm}^2 \text{ s}^{-1}$	1.870	2.479	2.867	1.892	1.030

Table S4. Comparison of the electrochemical performances of 0.02CrMO with recently reported manganese oxide electrodes.

Electrode/Mass loading/mg cm ⁻²	Operatin g voltage/V	Specific capacitance/F g ⁻¹	Rate capability/%	Capacitance retention/%	Referenc e
Al-doped MnO ₂ /4	0-0.8	213 at 0.1 A g ⁻¹	51.6% (0.1-5 A g ⁻¹)	91% (15000 cycles at 2 A g ⁻¹)	1
Fe-doped MnO ₂ /10-12	-0.1-0.9	175.6 at 5 mV s ⁻¹	47.7% (5-100 mV s ⁻¹)	79.7% (6000 cycles at 50 mV s ⁻¹)	2
D-MnO ₂ (defective MnO ₂)/2	0-0.8	202 at 1 A g ⁻¹	68.3% (1-20 A g ⁻¹)	89.4% (4000 cycles at 5 A g ⁻¹)	3
NNA ^a @MnO ₂ /3.51	0-0.8	214 at 1 mV s ⁻¹	- ^b	103.7% (20000 cycles at 10 mA cm ⁻²)	4
MnO ₂ @CNTF ^c /5.8	0-0.8	~192 at 1 A g ⁻¹	21% (1-10 A g ⁻¹)	- ^b	5
MnO _x -h/8.9	0-1.0	187.5 at 5 mV s ⁻¹	53% (5-100 mV s ⁻¹)	91% (6000 cycles at 200 mV s ⁻¹)	6
Na-MnO ₂ @CNTFs ^c /-	0-1.2	- ^b	70% (1-10 mA cm ⁻²)	92.1% (5000 cycles at 2 mA cm ⁻²)	7
Ni _{0.25} Mn _{0.75} O@C/NF ^d /-	0-1.4	- ^b	25% (1-16 mA cm ⁻²)	73% (5000 cycles at 2 mA cm ⁻²)	8
PMO/4.8	0-0.8	- ^b	- ^b	85.1% (10000 cycles at 10 A g ⁻¹)	This work
PMO/4.5	0-1.2	178 at 0.2 A g ⁻¹	54% (5-100 mV s ⁻¹) 38% (0.2-10 A g ⁻¹)	69.1% (10000 cycles at 10 A g ⁻¹)	
0.02CrMO/4.7	0-0.8	- ^b	- ^b	96.3% (10000 cycles at 10 A g ⁻¹)	

0.02CrMO/5.2	0-1.2	250 at 0.2 A g⁻¹	68% (5-100 mV s⁻¹)	95.4/82.6% (10000/30000 cycles at 10 A g⁻¹)
			50% (0.2-10 A g⁻¹)	

a NNA: Ni nanowire array; b “-”: no available literature data; c CNTF: carbon nanotube fiber; d NF: Ni foam.

References

1. Z. Hu, X. Xiao, C. Chen, T. Li, L. Huang, C. Zhang, J. Su, L. Miao, J. Jiang and Y. Zhang, *Nano Energy*, 2015, **11**, 226-234.
2. H. Liu, W. Gu, B. Luo, P. Fan, L. Liao, E. Tian, Y. Niu, J. Fu, Z. Wang and Y. Wu, *Electrochim. Acta*, 2018, **291**, 31-40.
3. Y.-P. Zhu, C. Xia, Y. Lei, N. Singh, U. Schwingenschlögl and H. N. Alshareef, *Nano Energy*, 2019, **56**, 357-364.
4. C. Xu, Z. Li, C. Yang, P. Zou, B. Xie, Z. Lin, Z. Zhang, B. Li, F. Kang and C.-P. Wong, *Adv. Mater.*, 2016, **28**, 4105-4110.
5. X. Li, L. Xiang, X. Xie, C. Zhang, S. Liu, Z. Li and J. Shen, *Nanotechnology*, 2020, **31**, 215406.
6. Y. Song, T. Liu, B. Yao, M. Li, T. Kou, Z.-H. Huang, D.-Y. Feng, F. Wang, Y. Tong, X.-X. Liu and Y. Li, *ACS Energy Lett.*, 2017, **2**, 1752-1759.
7. W. Zuo, C. Xie, P. Xu, Y. Li and J. Liu, *Adv. Mater.*, 2017, **29**, 1703463.
8. H. Jia, Y. Cai, J. Lin, H. Liang, J. Qi, J. Cao, J. Feng and W. Fei, *Adv. Sci.*, 2018, **5**, 1700887.